

Novel Properties of DDAB: Matrix Effect and Interaction with Oleate

Chris F. Thomas[†] and Pier Luigi Luisi^{*,‡}

Institut für Polymere, ETH-Zentrum, Universitätsstrasse 6, CH-8092 Zurich, Switzerland and Dipartimento di Biologia, Università degli studi Roma Tre, Viale Guglielmo Marconi 446, 00146 Rome, Italy

Received: December 31, 2003

We report an investigation on the interaction of the positively charged surfactant DDAB (didodecyldimethylammonium bromide) with preformed vesicles from POPC (1-palmitoyl-2-oleoyl-*sn*-glycero-3-phosphocholine). Addition of 1.9 mM DDAB to preformed POPC vesicles of different concentrations results in mixed vesicles, owing to the avid uptake of DDAB by POPC. This leads to the so-called matrix effect: when preformed POPC liposomes with a narrow size distribution are present in the aqueous solution, there is a fast formation process of mixed vesicles and the final size distribution closely resembles that of the preformed POPC liposomes. The final mixed vesicle system is stable in size and size distribution. The effect is independent of the initial size of the POPC vesicles and requires low relative concentrations of POPC with respect to DDAB (up to 1:4). Aside this, we report about the time stability of DDAB vesicles as a function of the aqueous buffer ionic strength and we investigate the interaction between negatively charged surfactant oleate and DDAB. The formation of mixed vesicles is observed, whose size distribution is strongly dependent on the mixing ratio of the two surfactants. Interestingly, the mixing of DDAB and oleate vesicles for values of DDAB molar fraction close to 0.4 leads to a very narrowly distributed vesicular species centered around 100 nm.

Introduction

In the past few years, we have devoted much attention to the spontaneous vesiculation of negatively charged surfactants, in particular, oleate and its mixed vesicles with phospholipids.^{1–4} We have studied in detail two novel features. One is the so-called matrix effect: a concentrated surfactant suspension added to an aqueous solution usually gives rise to a very broad size distribution of vesicles, but when the aqueous solution contains already preformed narrowly distributed vesicles (as obtained by extrusion), then the addition of fresh surfactant produces vesicles of about the same size as the preformed ones.^{1–4} This takes place when fresh oleate is added to either preformed oleate or POPC vesicles. The overall process corresponds to a kind of reproduction of vesicles of the same size, and it has been recently proposed that this might be relevant as prebiotic mechanism for the protocellular processes in the origin of life.^{5,6} Also, fusion processes between oleate and POPC vesicles and other types of vesicle-forming surfactants have been recently reported.⁷

The case of the positively charged DDAB is particularly important, given the fact that this compound is one of the most used in this field and also in medical applications.^{8–10} We will explore this case and study the interaction between positively and negatively charged vesicles (DDAB/oleate) in regard to the dependence of the size distribution on the ratio in the mixture. We apply laser dynamic light scattering (DLS) and electron microscopy to study the size and size distribution of the vesicles.

Results and Discussion

I: Stability of DDAB Vesicles. In this section, we discuss the stability of extruded DDAB vesicles by following the

changes of the average radius and the P-index (the polydispersity index, see Materials and Methods) by DLS with time and compare the behavior of the vesicles in water and 0.2 M sodium borate buffer (pH 8.5). The 5 mM DDAB suspensions were extruded through polycarbonate filters of pore radii 25 nm, 50, 100, and 200 nm. Figure 1a shows the results of the vesicle stability in water.

First of all, notice that the initial sizes of the vesicles after extrusion through large pores are smaller than the corresponding pore radii, especially for the 100-nm and 200-nm vesicles (vesicles being extruded through 100- and 200-nm pore radii, respectively). On the contrary, extrusion through smaller pores (25-nm radius) led to slightly larger particles, probably because of reversible vesicle deformation processes.¹¹ Altogether, the vesicles were stable with time not showing tremendous growing even after 75 days of storage. Kondo et al. have already reported that sonicated DDAB vesicles in water in the range of 10–20 nm remained stable for at least 14 days.¹² In borate (Figure 1b), the initial sizes were even smaller than in water, significantly smaller than the pore radii, and showed a recognizable mean size increase especially in the first 10 days after extrusion.

To rationalize these effects, one should keep in mind that the constraints imposed by the extrusion pore filters can be modified by the inherent thermodynamic stability of the vesicles and by the fact that vesicles smaller than the pore size pass anyway through. In addition, the dielectric constant of the solvent will play a role and there will be different hydration shells around the vesicles. In borate, the head–head interaction is supposed to change according to the counterion (Br^- versus $\text{HBO}_3^{2-}/\text{H}_2\text{BO}_3^-$) and interaction between Na^+ and Br^- ions is expected. In Figure 2a and 2b, the corresponding changes of the P-indices are shown.

From Figure 2a and 2b, it is apparent that there is a time-induced broadening of the size distribution for all vesicle radii.

* Address correspondence to this author.

[†] Institut für Polymere.

[‡] Università degli studi Roma Tre.

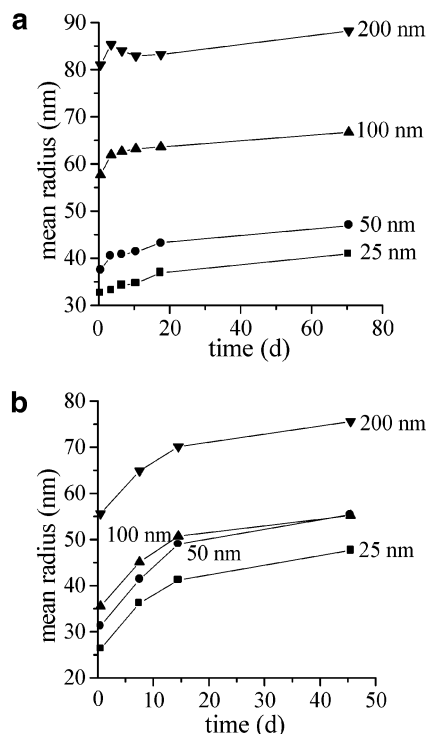


Figure 1. a. DLS of 5 mM DDAB vesicles in water, mean radius vs time for four different vesicle sizes, scattering angle 90° , 25.0°C . b. DLS of 5 mM DDAB vesicles in 0.2 M borate buffer (pH 8.5), mean radius vs time for four different vesicle sizes, scattering angle 90° , 25.0°C .

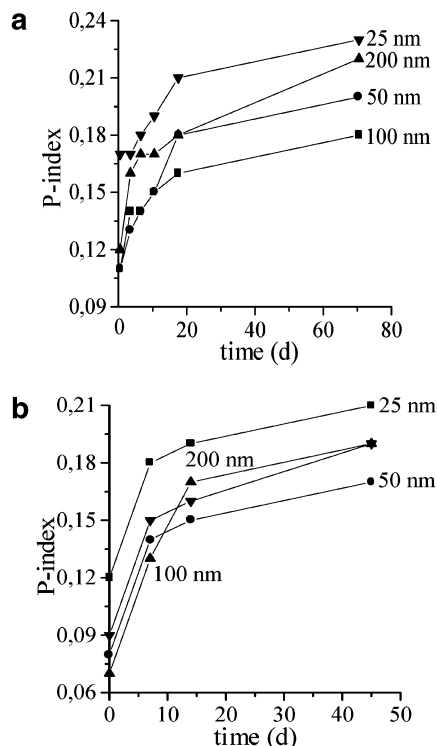


Figure 2. a. DLS of 5 mM DDAB vesicles in water, P-index vs time for four different vesicle sizes, scattering angle 90° , 25.0°C . b. DLS of 5 mM DDAB vesicles in 0.2 M borate buffer (pH 8.5), P-index vs time for four different vesicle sizes, scattering angle 90° , 25.0°C .

Interestingly, the fact that in water the increase in polydispersity was not accompanied by a significant increase of mean size suggests that both smaller and larger particles must have been formed. In both cases, the highest values for P-index were

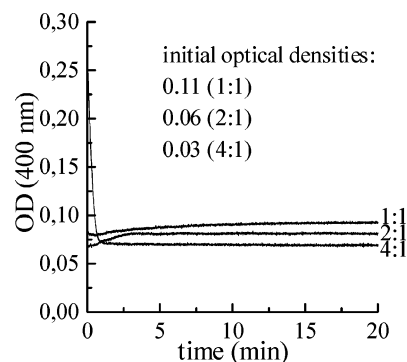


Figure 3. Effect of pre-added 25-nm POPC vesicles on the aggregation of DDAB after injection from 200 mM ethanol solution in borate buffer (0.2 M, pH 8.5). Optical density patterns at $\lambda = 400\text{ nm}$ and 25.0°C for 1.9 mM DDAB with 1.9 mM pre-added POPC (1:1), 1.9 mM DDAB with 0.95 mM pre-added POPC (2:1), 1.9 mM DDAB with 0.47 mM pre-added POPC (4:1).

obtained after extrusion through 25-nm pores which might be due to the effect of vesicle deformation.¹¹ The lowest values for P-index were obtained for 100-nm vesicles in water and 50-nm vesicles in borate which could be explained by the obvious preference of DDAB to generate smaller particles after the extrusion procedure in solutions of higher ionic strength. In borate, there was a stronger broadening of the size distribution accompanied with a clear growth of the mean size so that the distribution must have been enlarged especially in the direction of larger particles. If one compares the time evolution of the vesicles sizes from Figure 1a and 1b, it appears that the DDAB vesicles in borate buffer tended to acquire approximately the larger radii of those in water. Summarizing, extruded DDAB vesicles in borate turned out to be less stable than in water.

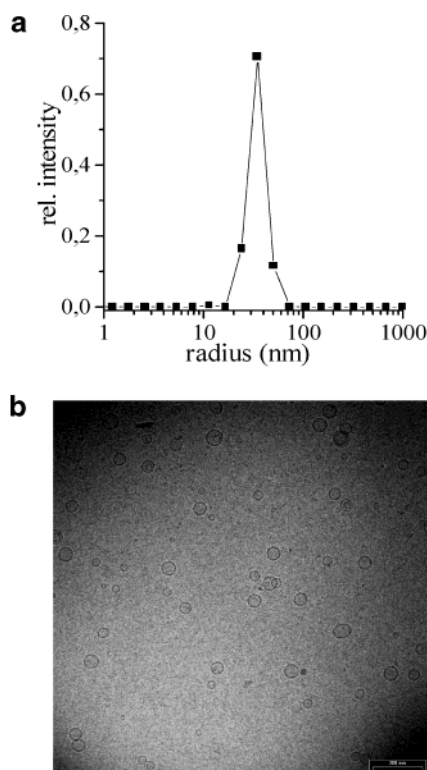
II: Matrix Effect. Let us consider now the matrix effect with DDAB. We already investigated the effect in negatively charged and neutral systems with oleate and POPC vesicles^{1–4} but not with positively charged surfactant. We have mentioned that in the spontaneous vesiculation of oleate two features were observed, one having to do with the sigmoid time progress of vesicle formation leading to a polydisperse vesicular population and the other with the matrix effect. The latter one concerns the influence of pre-added extruded vesicles on the aggregation of added surfactant, whereby the resulting vesicles show a size and size distribution that are comparable to those of the pre-added ones.^{1–4} In the following section, we report the size-determining effect of pre-added POPC vesicles and in respect of illustration we apply electron microscopy and DLS to the samples.

Extruded POPC vesicles of different radii (25-nm and 50-nm POPC) and different concentrations were used as pre-added vesicles, and DDAB was added from ethanol solution. Conditions were such that three different final concentrations in DDAB (1.9 mM, 0.95 mM, and 3.8 mM) were obtained. Let us consider first the results with a final concentration in DDAB of 1.9 mM in the presence of 25-nm POPC vesicles. When DDAB from ethanol stock solution was added to equimolar 25-nm POPC vesicles of average size 35.2 nm ($\pm 0.2\text{ nm}$ standard deviation) and P-index 0.03 (± 0.01 standard deviation), a fast formation process of mixed vesicles was observed (see Figure 3) and the final vesicle system was stable with time. Notice from Figure 3 (see also Table 1) that a low final optical density was observed, suggesting that a rather narrow size distribution of small aggregates has been obtained, similar to that of the pre-added POPC vesicles.

TABLE 1: Results of Matrix Effect Experiments with Different Concentrations of Pre-Added 25-nm POPC Vesicles and Final Concentration 1.9 mM in DDAB, Optical Density, P-Index, and Vesicle Size

expt	[DDAB] (mM)	[POPC] (mM)	ratio ^a	i. OD ^b	f. OD ^c	i. size ^d (nm)	f. size ^e (nm)	i. P ^f	f. P ^g	size change ^h (%)
1	1.9	3.8	1:2	0.21	0.14	34.8	28.0	0.04	0.09	-20
2	1.9	1.9	1:1	0.11	0.09	35.2	30.5	0.03	0.08	-13
3	1.9	0.95	2:1	0.06	0.08	35.5	33.4	0.03	0.09	-6
4	1.9	0.47	4:1	0.03	0.07	37.4	37.9	0.06	0.11	1

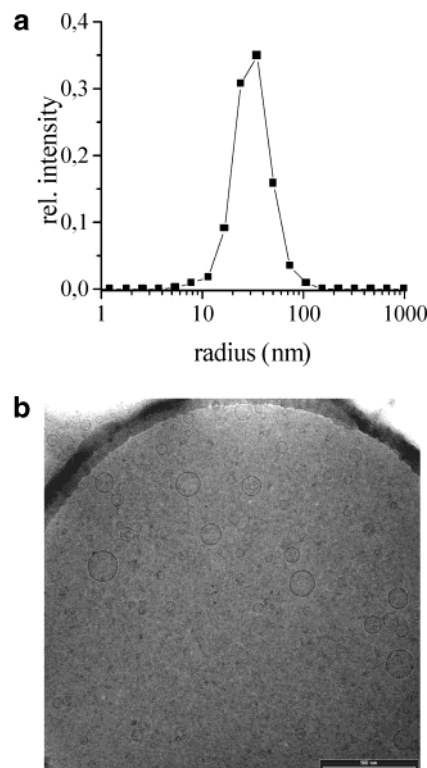
^a Ratio of [DDAB]/[POPC]. ^b Initial optical density (pre-added POPC vesicles). ^c Final optical density (for mixed POPC/DDAB vesicles). ^d Initial size (pre-added POPC vesicles). ^e Final size (mixed POPC/DDAB vesicles). ^f Initial P-index (pre-added POPC vesicles). ^g Final P-index (mixed POPC/DDAB vesicles). ^h Size change obtained by f. size/i. size.

**Figure 4.** a. DLS size distribution of 1.9 mM 25-nm POPC in 0.2 M borate buffer (pH 8.5), 25.0 °C, mean radius 35.2 nm, P-index 0.03, scattering angle 90°. b. Cryo-TEM micrograph of 1.9 mM 25-nm POPC in 0.2 M borate buffer (pH 8.5), bar represents 200 nm.

The fast formation is observed also in mixtures containing DDAB in excess. From Figure 3 (4:1 DDAB excess), there is evidence of intermediary large aggregates as indicated by the high initial optical density after the injection. As typical for the matrix effect, the resulting mixed vesicle population (see Figure 5a and b) showed a mean radius of 30.5 nm (± 0.2 nm) and a P-index of 0.08 (± 0.01), similar to the pre-added POPC vesicles (see Figure 4a and b).

The overall final surfactant concentration in this experiment is twice as high as at the beginning. Table 1 shows the results obtained by matrix effect experiments with different ratios of DDAB to pre-added POPC vesicles.

It is apparent that the presence of pre-added POPC vesicles influenced the size and size distribution of the final mixed vesicles up to a ratio of at least 4:1 in favor of DDAB. Further reduction of the POPC fraction led to the disappearance of the matrix effect accompanied by strong particle growth and broadening of the mixed vesicle size distribution. The electron

**Figure 5.** a. DLS size distribution of 1.9 mM 25-nm POPC in 0.2 M borate buffer (pH 8.5), 25.0 °C, after addition of DDAB from 200 mM stock solution (final concentration 1.9 mM), scattering angle 90°. b. Cryo-TEM micrograph of 1.9 mM 25-nm POPC in 0.2 M borate buffer (pH 8.5), after addition of DDAB from 200 mM stock solution (final concentration 1.9 mM), bar represents 500 nm.**TABLE 2: Results of Matrix Effect Experiments with Different Concentrations of Pre-Added 50-nm POPC Vesicles and Final Concentration 1.9 mM in DDAB, Change of Optical Density, P-Index, and Vesicle Size**

expt	[DDAB] (mM)	[POPC] (mM)	ratio ^a	i. size ^b (nm)	f. size ^c (nm)	i. P ^d	f. P ^e	size change ^f (%)
1	1.9	1.9	1:1	60.7	60.1	0.06	0.08	-1
2	1.9	0.47	2:1	57.3	59.4	0.05	0.1	4
3	1.9	0.23	4:1	57.9	70.2	0.04	0.12	21

^a Ratio of [DDAB]/[POPC]. ^b Initial size (pre-added POPC vesicles). ^c Final size (mixed POPC/DDAB vesicles). ^d Initial P-index (pre-added POPC vesicles). ^e Final P-index (mixed POPC/DDAB vesicles). ^f Size change obtained by f. size/i. size.

micrograph shows that after DDAB addition (Figure 5b) there is evidence of larger mixed vesicles and simultaneously of a fraction of smaller ones—in agreement with the DLS results. Above this, the micrographs confirm that both populations consist of spherical particles (a necessary prerequisite for a simple elaboration of DLS data). Counting and sizing from several micrographs provided results very similar to DLS but slightly shifted to smaller radii. This effect is caused by the higher scattering efficiency of larger particles and by the fact that DLS—in contrast to an electron micrograph where the solvent layer is “invisible”—gives the hydrodynamic radius of the vesicles. Analogous results were obtained in the 50-nm pre-added POPC vesicles as reported in Table 2.

With pre-added POPC vesicles having a mean radius of 60.7 nm (± 0.3 nm), the final vesicles (with a double final overall concentration) maintained almost the same size (60.1 nm (± 0.3 nm)). Also, the size distribution remained quite narrow (pre-added POPC vesicles: P-index 0.06 (± 0.01), final mixed POPC/DDAB vesicles: P-index 0.08 (± 0.01)). The fact that also in

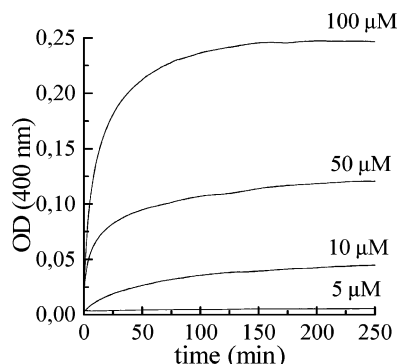


Figure 6. Formation of mixed DDAB/oleate vesicles in 0.2 M borate buffer at pH 8.5, 25.0 °C, optical density patterns at $\lambda = 400$ nm shown for 5 μ M DDAB + 5 μ M oleate, 10 μ M DDAB + 10 μ M oleate, 50 μ M DDAB + 50 μ M oleate, 100 μ M DDAB + 100 μ M oleate.

this case the final size depends on the initial size can be taken as an indication that the effect is not just confined to the small vesicles and that the mixed vesicles do not favor a certain size being thermodynamically more stable than the others.

We also performed matrix effect experiments at a final concentration of 0.95 mM in DDAB and observed similar results. Once again there was a strong effect of the pre-added POPC vesicles on the properties of the final mixed system and the size and size distribution were clearly transferred from the first to the second vesicle generation up to a DDAB/POPC ratio of 4:1. Finally, we performed experiments at a DDAB concentration as high as 3.8 mM and received similar results so that one can conclude that both surfactant concentrations are variable without losing the effect.

III: Effect of DDAB on Oleate Vesicles. In the last 15 years, several catanionic systems have been investigated either in regard to theoretical investigations,²⁵ phase diagrams,^{16–24} or other features such as kinetics, mechanisms of vesicle formation, and preparation techniques.^{21,26–32} In particular, the existence of pure vesicular phases in mixed catanionic systems has been reported.^{16–18,20,22,23,31} Vesicles from these phases were of high stability but rather polydisperse size distribution,^{16,17,22,24} and above this it was observed that the size distribution can become narrower within a vesicular phase.^{16,17,20}

Let us consider now the new system consisting of oleate and DDAB. Figure 6 illustrates an experiment in which the aggregation of these oppositely charged surfactants is attempted by mixing separated samples of oleate and DDAB to each other under gentle stirring.

Apparently, the process needed a couple of hours for reaching a plateau but even from 5 μ M solutions a formation process was observable, suggesting that mixed vesicles were formed with a very low critical concentration. However, at higher concentrations (200 μ M), macroscopic flocculation was observed (data not shown). Another feature concerning the size distribution of DDAB/oleate vesicles as a function of their mixing ratio is shown in Figure 7, which reports in particular the P-index phase diagram of the system, obtained by mixing together given volumes of 1 mM samples under gentle stirring. In Figure 8, the corresponding size distributions for a series of molar fractions of DDAB are shown.

Let us consider now the interaction between oleate and DDAB at different molar fractions of DDAB in regard to the effect on the size distribution of the mixed vesicles. As can be seen in Figure 8, the size distribution of pure 1 mM oleate in borate buffer is very broad, extending from small vesicles of around 10 nm up to large aggregates of more than 1000 nm. Addition

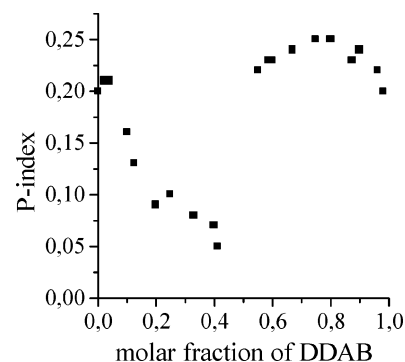


Figure 7. P-index phase diagram (from DLS) for DDAB/oleate mixtures, total concentration 1 mM in 0.2 M borate buffer at pH 8.5, 25.0 °C, scattering angle 90°.

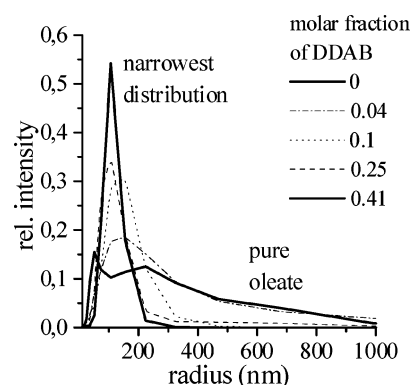


Figure 8. Size distributions (from DLS) for DDAB/oleate mixtures, total concentration 1 mM in 0.2 M borate buffer at pH 8.5, 25.0 °C, scattering angle 90°.

of DDAB to this very broad size distribution gave rise to a very sharp and narrow distribution of mixed vesicles, as illustrated in Figure 8, with a peak centered at about 100 nm. The strong dependence on the ratio in the mixture is best illustrated in Figure 7, showing in particular the progressive narrowing of the mixed vesicles size distribution with increasing amount of DDAB. Up to a DDAB molar fraction of 0.41, the P-index decreases sharply, that is, it is as if the addition of DDAB has the general effect of producing mixed vesicles with a more and more narrow size distribution. These vesicular species were very stable with time for at least 3 months. Between DDAB molar fractions of 0.41 and 0.60, flocculation occurred, namely, the mixed vesicular system was no longer thermodynamically stable which is in agreement with other catanionic systems.^{16,17,20} Above a DDAB molar fraction of 0.60, the P-index remains at rather high levels, and there is no sharpening of the size distribution. To explain this observation, one should think also in terms of the composition of the mixture^{33,34} and the surfactant packing parameters. Figure 8 shows also the DLS result of the narrowest size distribution obtained at a DDAB molar fraction of 0.41. Comparison of this pattern with Figure 4a confirms that mixed vesicle formation processes can generate catanionic populations being nearly as narrowly distributed as populations of extruded vesicles.

Concluding Remarks

The most general observation stemming from these studies is that many of the salient features observed for the negatively charged oleate vesicles hold true also for the positively charged DDAB. This is particularly so as far as the interaction with phospholipid vesicles is concerned and for the matrix effect. The analogy of behavior between oleate and DDAB, at first

sight surprising, can be explained mostly by the consideration that the hydrophobic effect more than the charge is responsible for the observed physicochemical effects. Beyond this general consideration, the rationalization of the mechanism is however difficult, as too many parameters appear to play a role in determining the rate of the processes, the type of size distribution, the form of the curves, and so forth. Concerning the interaction between POPC and DDAB, it seems that the phospholipid system has a natural strong tendency to incorporate long-chain surfactants regardless of the charge. The fact that in both cases this tendency results in the matrix effect, namely, in the multiplication of mixed vesicles having a size distribution very close to that of the "germ" liposomes, is still a very interesting and surprising feature that requires a deeper inquiry. It has been recently postulated that this kind of feature might have been of relevance in prebiotic times as a mechanism of replication of protocells of a given narrowly distributed size.⁵

The fact that the size distribution in a system of mixed DDAB/oleate surfactant is strongly dependent on the composition of the mixture and that in a certain ratio it gives rise to an almost monodisperse size distribution was perhaps the most surprising result of this investigation. Apparently, in the composition range around 0.4 molar fraction of DDAB, the size distribution is the narrowest and thermodynamically most stable, whereas at a 50:50 ratio there is flocculation and a complete loss of the vesicular system stability. All these novel features indicate on one hand that the field of vesicles may still be rich of interesting surprises, and on the other hand these novel features appear difficult to rationalize in simple terms, pointing to the inherent complexity of these systems.

Materials and Methods

Chemicals. Oleic acid (*cis*-9-octadecenoic acid), boric acid, ethanol, and DDAB (didodecyltrimethylammonium bromide) were from Fluka, (Buchs, Switzerland). Sodium hydroxide was from Synopharm, (Schweizerhall, Switzerland) and POPC (1-palmitoyl-2-oleoyl-*sn*-glycero-3-phosphocholine) was from Avanti Polar Lipids (Alabaster, AL). All aqueous solutions were prepared in fresh deionized water, obtained by a Milli-Q (Millipore) apparatus (Volketswil, Switzerland).

Turbidity Measurements. Turbidity (optical density) measurements were carried out at 25.0 °C recording the absorbance at 400 nm under gentle magnetic stirring in cell, with a Cary 1E UV/visible spectrophotometer from Varian, Australia. Quartz cells with path length of 1 cm were used and the sample volume was chosen to 2.5 mL except experiments concerning reactions between DDAB and oleate (2 mL).

Electron Microscopy. Electron micrographs were prepared in the laboratory of electron microscopy I at the ETH Zürich using the cryo-fixation method.

Dynamic Light Scattering Measurements. Determination of vesicle size (hydrodynamic radius) and size distribution was done by DLS with a photocalibration spectrometer consisting of a 25 mW He–Ne laser (Model 127, Spectra-Physics Lasers, Mountain View, Canada), an ALV DLS/SLS-5000 Compact Goniometer System (ALV, Langen, Germany), two SPCM-AQR avalanche photodiodes (PerkinElmer Optoelectronics, Vaudreuil, Canada), and an ALV-5000 Multiple-tau Digital Correlator (ALV, Langen, Germany). The scattering cells were immersed in a thermostated bath at 25.0 °C. Measurements and analysis were performed at scattering angles of 60°, 90°, and 120° whereas just the results obtained at 90° are shown. Data were analyzed according to (a) the cumulant method, which provides values for mean radius (the so-called *z*-average) and the

polydispersity index (P-index) and (b) the Laplace inversion procedure, using CONTIN as preferred algorithm. In both cases, results are intended as average of 10 independent measurements of the same sample. The P-index is an indicator for the width of the size distribution; low values indicate narrow, relatively monodisperse populations. Size distributions are reported in terms of relative intensity, that is, large particles are overestimated.

POPC Vesicles. POPC vesicles for matrix effect experiments were prepared by applying the film method. A quantity of 38 mg solid POPC was dissolved in 3 mL of chloroform in a round-bottomed flask followed by removing the solvent by evaporation (Büchi Rotavapor) and high vacuum-drying of the film overnight. The film was then dispersed by vigorous shaking in 10 mL of 0.2 M sodium borate buffer (pH 8.5), giving a 5 mM suspension. Freeze-and-thaw cycles were applied to the samples using liquid nitrogen for reducing the lamellarity of the vesicles.³⁵ Then, the suspensions were extruded (Extruder, Lipex Biomembranes, Vancouver, Canada) through two stacked polycarbonate filters (Nuclepore, Sterico AG, Dietikon, Switzerland) starting with 200-nm pore radius followed by 100, 50, and 25 nm; any extrusion step was repeated 10 times. Afterward, the suspensions were diluted according to the experimental setup.

DDAB Vesicles. *Method i.* For vesicle stability experiments, 34.7 mg solid DDAB were dispersed in either 15 mL water or 0.2 M borate buffer (pH 8.5) giving 5 mM dispersions followed by stirring and freeze-and-thaw cycles. Extrusion was applied to the vesicles from pore radius 200 nm to 25 nm in the way as described above.

Method ii. In the experiments concerning investigations of the matrix effect, injection method was applied. A 200 mM concentrated stock solution of DDAB was prepared by dissolving solid DDAB in ethanol. The solution was injected with an Eppendorf pipet into suspensions of POPC (in 0.2 M borate buffer, pH 8.5), always followed by shaking three times by hand. To obtain a final concentration of 1.9 mM in DDAB, an aliquot of 23.7 μ L of the 200 mM stock solution was injected giving a sample volume of 2.5 mL. Accordingly, final concentrations of 0.95 mM and 3.8 mM in DDAB were obtained by equivoluminal injection from 100 mM and 400 mM ethanol stock solutions, respectively, keeping constant the ethanol volume fraction in all experiments at 0.95%.

Mixed DDAB/Oleate Vesicles. Experiments dealing with mixed vesicles were performed by first preparing separate 1 mM suspensions of DDAB and oleate both in borate buffer. The DDAB suspension was prepared as described under method i without freeze-and-thaw application and then was diluted. Oleate vesicles were prepared as 5 mM suspensions by injection of 23.8 μ L of oleic acid into 15 mL of borate buffer followed by vigorous stirring and dilution. Kinetics of the reaction between samples of oleate and DDAB were followed spectrophotometrically by mixing together 1 mL of each sample into a quartz cell, followed by shaking three times by hand. Accordingly, samples of other ratios regarding measurements of the size distribution of the mixed vesicles were performed by mixing together different volumes of 1 mM suspensions of oleate and DDAB. The minor volume compound was always added to the excess compound under gentle stirring.

Acknowledgment. We thank Matthias Voser for his support in light microscopy and Martin Müller for providing the electron micrographs. Pasquale Stano is acknowledged for valuable comments on the paper.

References and Notes

- (1) Blöchliger, E.; Blocher, M.; Walde, P.; Luisi, P. L. *J. Phys. Chem. B* **1998**, *102*, 10383–10390.
- (2) Lonchin, S.; Luisi, P. L.; Walde, P.; Robinson, B. H. *J. Phys. Chem. B* **1999**, *103*, 10910–10916.
- (3) Berclaz, N.; Müller, M.; Walde, P.; Luisi, P. L. *J. Phys. Chem. B* **2001**, *105*, 1056–1064.
- (4) Rasi, S.; Mavelli, F.; Luisi, P. L. *J. Phys. Chem. B* **2003**, *107*, 14068–14076.
- (5) Luisi, P. L.; Stano, P.; Rasi, S.; Mavelli, F. *Artificial Life*, in press.
- (6) Wick, R.; Walde, P.; Luisi, P. L. *J. Am. Chem. Soc.* **1995**, *117*, 1435–1436.
- (7) Cheng, Z.; Luisi, P. L. *J. Phys. Chem. B* **2003**, *107*, 10940–10945.
- (8) Jungerman, E. *Cationic Surfactants*; Marcel Dekker: New York, 1970.
- (9) Kunieda, H.; Shinoda, K. *J. Phys. Chem.* **1978**, *82*, 1710.
- (10) Lasic, D. D. *Liposomes: from Physics to Application*; Elsevier: Amsterdam, 1993.
- (11) Hunter, D. G.; Frisken, B. J. *Biophys. J.* **1998**, *74*, 2997.
- (12) Kondo, Y.; Abe, M.; Ogino, K.; Uchiyama, H.; Tucker, E. E.; Scamehorn, J. F.; Sherill, D. C. *Colloids Surf., B* **1993**, *1*, 53.
- (13) Marques, E. F.; Regev, O.; Khan, A.; Lindman, B. *Adv. Colloid Interface Sci.* **2003**, *100*, 89–91.
- (14) Dubois, M.; Zemb, Th. *Langmuir* **1991**, *7*, 1352–1354.
- (15) Caboi, F.; Monduzzi, M. *Langmuir* **1996**, *12*, 3548–3551.
- (16) Kondo, Y.; Uchiyama, H.; Yoshino, N.; Nishiyama, K.; Abe, M. *Langmuir* **1995**, *11*, 2380–2384.
- (17) Marques, E. F.; Regev, O.; Khan, A.; Maria da Graça, M.; Lindman, B. *J. Phys. Chem.* **1998**, *102*, 6747–6758.
- (18) Bergström, M.; Pedersen, J. S. *Langmuir* **1999**, *15*, 2250–2253.
- (19) Marques, E.; Khan, A.; Maria da Graça, M.; Lindman, B. *J. Phys. Chem.* **1993**, *97*, 4729–4736.
- (20) Kaler, E. W.; Murthy, A. K.; Rodriguez, B. E.; Zasadzinski, J. A. *N. Science* **1989**, *245*, No. 4924, 1371–1374.
- (21) O'Connor, A. J.; Hatton, T. A.; Bose, A. *Langmuir* **1997**, *13*, 6931–6940.
- (22) Horbaschek, K.; Hoffmann, H.; Hao, J. *J. Phys. Chem. B* **2000**, *104*, 2782.
- (23) Koehler, R. D.; Raghavan, S. R.; Kaler, E. W. *J. Phys. Chem. B* **2000**, *104*, 11035.
- (24) Caria, A.; Khan, A. *Langmuir* **1996**, *12*, 6282–6290.
- (25) Jung, H. T.; Coldren, B.; Zasadzinski, J. A.; Iampietro, D. J.; Kaler, E. W. *Proc. Natl. Acad. Sci. USA* **2001**, *98*, 1353–1357.
- (26) Stamatis, L.; Leventis, R.; Zuckermann, M. J.; Silviu, J. R. *Biochemistry* **1988**, *27*, 3919.
- (27) Shioi, A.; Hatton, T. A. *Langmuir* **2002**, *18*, 7341–7348.
- (28) Marques, E. F. *Langmuir* **2000**, *16*, 4798–4799, 4801–4802.
- (29) Marchi-Artzner, V.; Ludovic, J.; Belloni, L.; Raison, D.; Lacombe, L.; Lehn, J.-M. *J. Phys. Chem. B* **1996**, *100*, 13850.
- (30) Caillet, C.; Hebrant, M.; Tondre, C. *Langmuir* **2000**, *16*, 9099–9102.
- (31) Fukada, H.; Kawata, K.; Okuda, H. *J. Am. Chem. Soc.* **1990**, *112*, 1635–1637.
- (32) Salkar, R. A.; Mukesh, D.; Samant, S. D.; Manohar, C. *Langmuir* **1998**, *14*, 3778–3782.
- (33) We are not dealing with pure negatively charged oleate vesicles but with mixed sodium oleate/oleic acid vesicles with about 50% of the surfactant molecules present in the deionized form.
- (34) Cistola, D. P.; Hamilton, J. A.; Jackson, D.; Small, D. M. *Biochemistry* **1988**, *27*, 1881–1884.
- (35) MacDonald, R. C.; MacDonald, R. I. Chapter 13: Applications of freezing and thawing in liposome research. In *Liposome Technology-Volume I*; Gregoriadis, G., Ed.; CRC Press: Boca Raton, FL, 1993; pp 209–223.